Hindawi
Mathematical Problems in Engineering
Volume 2022, Article ID 3029932, 17 pages
https://doi.org/10.1155/2022/3029932

Research Article

Discrete Generalized Inverted Exponential Distribution: Case Study Color Image Segmentation

Mohamed Abd Elaziz,[1,2,3] **Nahla S. Abdelrahman**,[2] **N. A. Hassan**,[2] **and M. O. Mohamed**[2]

[1]*Faculty of Computer Science and Engineering, Galala University, Suez 435611, Egypt*
[2]*Department of Mathematics, Faculty of Science, Zagazig University, Zagazig 44519, Egypt*
[3]*Artificial Intelligence Research Center (AIRC), Ajman University, Ajman, P.O. Box 346, UAE*

Correspondence should be addressed to Mohamed Abd Elaziz; abd_el_aziz_m@yahoo.com

Received 23 December 2021; Revised 26 January 2022; Accepted 2 February 2022; Published 23 March 2022

Academic Editor: Saeid Jafarzadeh Ghoushchi

We present in this paper a discrete analogue of the continuous generalized inverted exponential distribution denoted by discrete generalized inverted exponential (DGIE) distribution. Since, it is cumbersome or difficult to measure a large number of observations in reality on a continuous scale in the area of reliability analysis. Yet, there are a number of discrete distributions in the literature; however, these distributions have certain difficulties in properly fitting a large amount of data in a variety of fields. The presented **DGIE**(β, θ) has shown the efficiency in fitting data better than some existing distribution. In this study, some basic distributional properties, moments, probability function, reliability indices, characteristic function, and the order statistics of the new DGIE are discussed. Estimation of the parameters is illustrated using the moment's method as well as the maximum likelihood method. Simulations are used to show the performance of the estimated parameters. The model with two real data sets is also examined. In addition, the developed DGIE is applied as color image segmentation which aims to cluster the pixels into their groups. To evaluate the performance of DGIE, a set of six color images is used, as well as it is compared with other image segmentation methods including Gaussian mixture model, K-means, and Fuzzy subspace clustering. The DGIE provides higher performance than other competitive methods.

1. Introduction

In the field of reliability analysis, it is inconvenient or difficult to measure a lot of observations in nature on a continuous scale. For example, in many practical satiations [1–9], reliability data are measured in terms of the number of cases, runs, or the number of days left for patients with the deadly disease since therapy. For more examples in reliability and lifetime applications, see Meeker and Escobar [10]. There are ways to build up a discrete distribution that has been recognized [11].

Indeed, this technique has been widely applied to generate new discrete distributions for example [12–18] and references cited therein. Abouammoh and Alshingiti [19] introduced a shape parameter to the inverted exponential distribution to get the generalized inverted exponential (GIE) distribution. The GIE distribution is derived from the exponetiated Frechet distribution [20]. The hazard rate of the GIE distribution can be decreasing or increasing, based on its shape parameter. The GIE has effectiveness in modeling a lot of data and can be applied in several applications, such as horse racing, life testing, queues, and wind speeds [20]. Abouammoh and Alshingiti [19] show that the GIE distribution provides a better fit than Weibull, gamma, generalized exponential distribution, and gamma distribution. The GIE can be widely used in many fields, see for example, [21, 22]. However, there exist a number of discrete distributions in the literature; there are some limitations in these distributions in fitting a lot of data in many areas effectively, such as geometric, discrete Lindely, and discrete logistic distributions. There is still a need to develop new discretized distributions that are able to have

applications such as image segmentation. This motivated us to present a new distribution.

The presented distribution discrete generalized inverted exponential (DGIE) is constructed from a generalized inverted exponential distribution. Parameters are estimated using two methods, namely moments and maximum likelihood. The consistency of the estimated parameters is illustrated using simulation. Based on to two data sets the proposed distribution is more convenient to analyze the given data more than competitive distributions. The proposed distribution is applied in color segmentation which helps in clustering the pixels into their groups. The DGIE provides higher performance than other competitive methods.

The main contribution of the current study can be summarized as follows:

(1) Present a new distribution discrete generalized inverted exponential (DGIE) to avoid the limitations of other distributions

(2) Compute the basic distributional properties, moments, probability function, reliability indices, characteristic function, and the order statistics of DGIE

(3) Evaluate the applicability of DGIE by using it to improve the color segmentation

The paper is organized as follows: in Section 2, we introduce the **DGIE**(β, θ) distribution and mention statistical properties, as failure function, survival function. In addition, we list some additional properties of the proposed distribution such as moment generating function, moments, quantile, entropy, stress-strength, mean residual lifetime, and order statistics. We analyse the **DGIE**(β, θ) using two real data set in Section 3. Finally, the conclusion is mentioned in Section 4.

2. Materials and Methods

2.1. Discrete Generalized Inverted Exponential Distribution

Definition 1. A random variable X is said to have a discrete generalized inverted exponential distribution with parameter β ($\beta > 0$) and $= e^{-\lambda}$, $0 < \theta < 1$, if its probability mass function (PMF) has the form:

$$P(X = x) = \left(1 - \theta^{1/(x)}\right)^{\beta} - \left(1 - \theta^{1/(x+1)}\right)^{\beta}; x \in \mathbb{N}_0. \quad (1)$$

We denote this distribution as **DGIE**(β, θ). Figure 1 illustrates several examples of the probability mass function of **DGIE**(β, θ) distribution for various values of β and θ.

2.1.1. Cumulative Distribution Function. The cumulative distribution function CDF of **DGIE**(β, θ) is given by

$$F(x, \alpha, \theta) = 1 - S(x, \alpha, \theta) + P = 1 - \left(1 - \theta^{1/(x+1)}\right)^{\beta}, \quad (2)$$

where β ($\beta > 0$) and $= e^{-\lambda}$, $0 < \theta < 1$. Monotonic property simply, we find out

$$\frac{f_X(x+1;\beta,\theta)}{f_X(x;\beta,\theta)} = \frac{\left(1 - \theta^{1/(x+1)}\right)^{\beta} - \left(1 - \theta^{1/(x+2)}\right)^{\beta}}{\left(1 - \theta^{1/(x)}\right)^{\beta} - \left(1 - \theta^{1/(x+2)}\right)^{\beta}}, x \in \mathbb{N}_0 \beta(\beta > 0) \text{ and } \theta = e^{-\lambda}, 0 < \theta < 1. \quad (3)$$

Is a decreasing function of which leads to $\{f_X(x;\beta,\theta)\}^2 > f_X(x+1;\beta,\theta) f_X(x-1;\beta,\theta); x \in \mathbb{N}_0$ β ($\beta > 0$) and $\theta = e^{-\lambda}$, $0 < \theta < 1$.

The distribution is log-concave. Based on the log concavity (Mark, 1996), the proposed of **DGIE**(β, θ) distribution is unimodal with increasing failure rate distribution, and it all its moments.

Furthermore, the quantile function of **DGIE**(β, θ) distribution, say $Q(p)$, from $F(x_p) = p$, is given by

$$x_p = \frac{\ln \theta}{\ln\left(1 - (1 - p)^{1/\beta}\right)} - 1, \quad (4)$$

where β ($\beta > 0$), $\theta = e^{-\lambda}$, $0 < \theta < 1$ and $0 < p < 1$. Where n denotes the greatest integer function.

Hence the median can be obtained by putting $p = 1/2$ in equation (4)

$$\text{Med}(X) = \frac{\ln \theta}{\ln\left(1 - (1/2)^{1/\beta}\right)} - 1. \quad (5)$$

Survival function: The survival function of **DGIE**(β, θ) distribution is defined as

$$S(x, \beta, \theta) = P(X \geq x) = \left(1 - \theta^{1/x}\right)^{\beta}; \quad x \in \mathbb{N}_0. \quad (6)$$

Hazard rate, r(x) is put as

$$h(x, \beta, \theta) = \frac{p(x)}{s(x)} = \frac{\left(1 - \theta^{1/x}\right)^{\beta} - \left(1 - \theta^{1/(x+1)}\right)^{\beta}}{\left(1 - \theta^{1/x}\right)^{\beta}}; \quad x \in \mathbb{N}_0. \quad (7)$$

Figure 2 shows the HRF plots of **DGIE**(β, θ) distribution for various values of β and θ.

The reversed hazard rate function (RHRF) of the **DGIE**(β, θ) distribution is put in the form

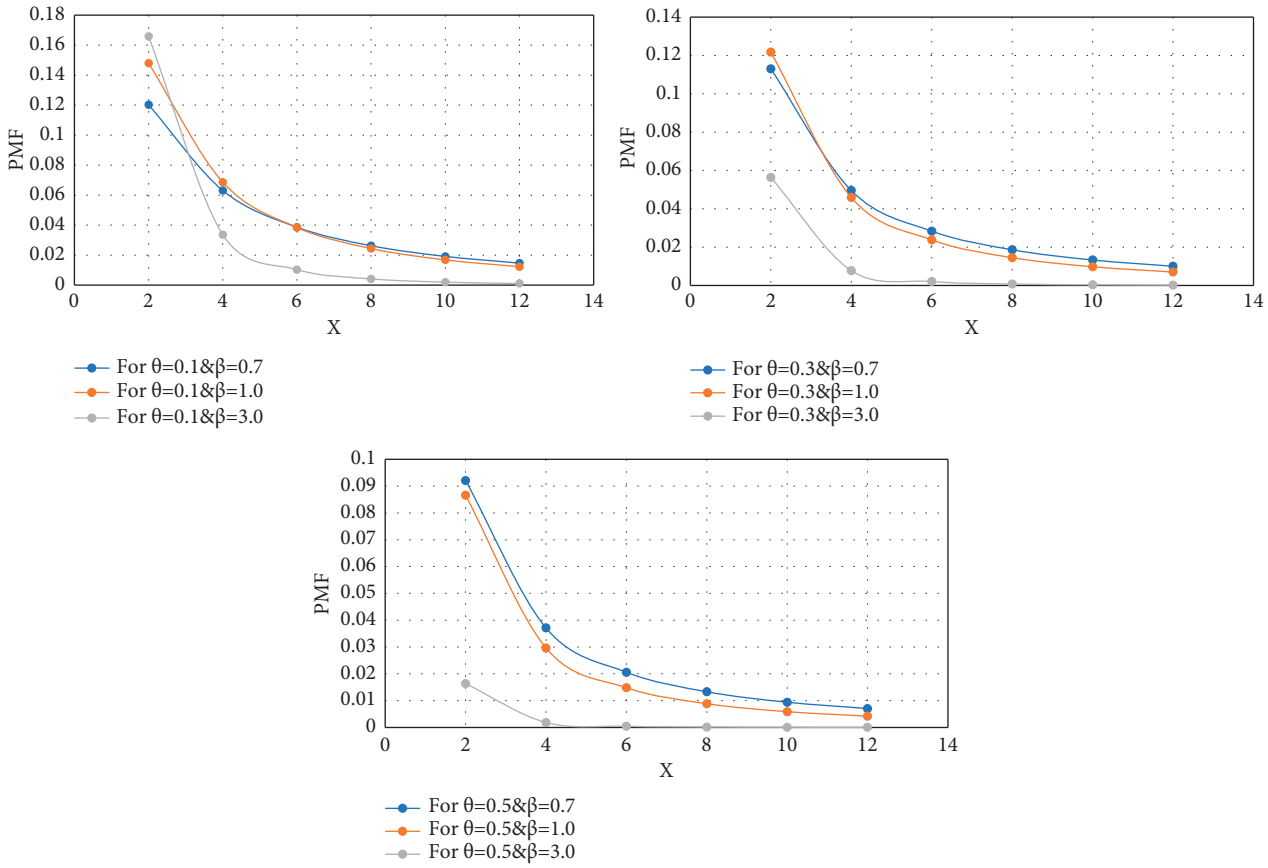

Figure 1: PMF of the **DGIE**(β, θ).

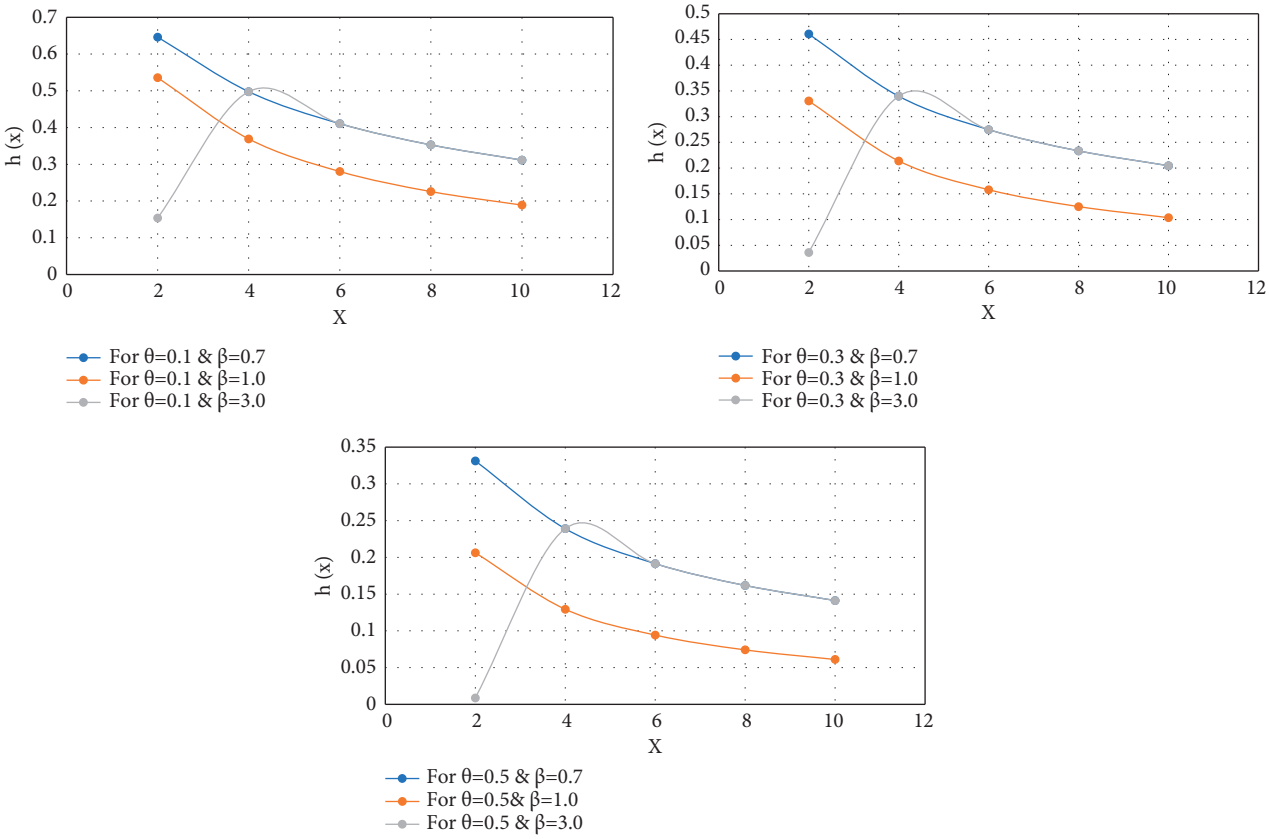

Figure 2: HRF of the **DGIE**(β, θ).

$$r(x,\beta,\theta)=\frac{\left(1-\theta^{1/x}\right)^{\beta}-\left(1-\theta^{1/(x+1)}\right)^{\beta}}{1-\left(1-\theta^{1/x}\right)^{\beta}};\ x\in\mathbb{N}_0. \tag{8}$$

Figure 3 indicate the RHRF plots of **DGIE**(β,θ) distribution for various values of β and θ.

2.2. Statistical Properties. The $\mathbf{r^{th}}$ moment $\mu_{\mathbf{r}}^{'}$ of a discrete exponentiated exponential distribution **DGIE**(β,θ) about the origin is obtained as follows:

$$\begin{aligned}\mu_r'&=\sum_{x=0}^{\infty}x^r\left[\left(1-\theta^{1/x}\right)^{\beta}-\left(1-\theta^{1/(x+1)}\right)^{\beta}\right],\\ \mu_r'&=E\left[X^r\right]=\sum_{x=0}^{\infty}x^rP(X=x).\end{aligned} \tag{9}$$

The moment generating function (MGF) $\mathbf{M_X(t)}$ of **DGIE**(β,θ) distribution is computed as follows:

$$\begin{aligned}M_X(t)&=E\left[e^{\mathrm{tx}}\right]=\sum_{x=0}^{\infty}e^{\mathrm{tx}}P(X=x)\\&=\sum_{x=0}^{\infty}e^{\mathrm{tx}}P(X=x)\left[\left(1-\theta^{1/x}\right)^{\beta}-\left(1-\theta^{1/(x+1)}\right)^{\beta}\right].\end{aligned} \tag{10}$$

The mean (μ) of DGIE(β,θ) distribution is derived as

$$\mu_1'=\mu=E[X]=\sum_{x=0}^{\infty}x\left[\left(1-\theta^{1/x}\right)^{\beta}-\left(1-\theta^{1/(x+1)}\right)^{\beta}\right]. \tag{11}$$

The second moment is obtained as

$$\mu_2'=\mu=E\left[X^2\right]=\sum_{x=0}^{\infty}x^2\left[\left(1-\theta^{1/x}\right)^{\beta}-\left(1-\theta^{1/(x+1)}\right)^{\beta}\right]. \tag{12}$$

Hence, the variance (σ^2) could be derived as

$$\mathrm{var}(X)=\sum_{x=0}^{\infty}x^2\left[\left(1-\theta^{1/x}\right)^{\beta}-\left(1-\theta^{1/(x+1)}\right)^{\beta}\right]-\left(\sum_{x=0}^{\infty}x\left[\left(1-\theta^{1/x}\right)^{\beta}-\left(1-\theta^{1/(x+1)}\right)^{\beta}\right]\right)^2. \tag{13}$$

The 3rd and 4th moments are, respectively are obtained as

$$\begin{aligned}\mu_3'&=E\left[X^3\right]=\sum_{x=0}^{\infty}x^3\left[\left(1-\theta^{1/x}\right)^{\beta}-\left(1-\theta^{1/(x+1)}\right)^{\beta}\right],\\ \mu_4'&=E\left[X^4\right]=\sum_{x=0}^{\infty}x^4\left[\left(1-\theta^{1/x}\right)^{\beta}-\left(1-\theta^{1/(x+1)}\right)^{\beta}\right].\end{aligned} \tag{14}$$

The measure of skewness α_3 of DGIE(β,θ) distribution is obtained as follows:

$$\begin{aligned}\alpha_3&=\frac{\mu_3'-2\mu_2'\mu+\mu^3}{\sigma^3}\\&=\frac{1}{\sigma^3}\left\{\left[\sum_{x=0}^{\infty}x^3\left[\left(1-\theta^{1/x}\right)^{\beta}-\left(1-\theta^{1/(x+1)}\right)^{\beta}\right]\right]-2\mu\sum_{x=0}^{\infty}x^2\left[\left(1-\theta^{1/x}\right)^{\beta}-\left(1-\theta^{1/(x+1)}\right)^{\beta}\right]\right\}+\frac{\mu^3}{\sigma^3}.\end{aligned} \tag{15}$$

The measure of kurtosis α_4 of DGIE(β,θ) distribution is obtained as follows:

$$\begin{aligned}\alpha_4&=\frac{\mu_4'-4\mu_3'\mu+6\mu_2'\mu^2-3\mu^4}{\sigma^4}\\ \alpha_4&=\frac{1}{\sigma^4}\left\{\sum_{x=0}^{\infty}x^4\left[\left(1-\theta^{1/x}\right)^{\beta}-\left(1-\theta^{1/(x+1)}\right)^{\beta}\right]-4\mu\sum_{x=0}^{\infty}x^3\left[\left(1-\theta^{1/x}\right)^{\beta}-\left(1-\theta^{1/(x+1)}\right)^{\beta}\right]\right.\\&\left.+6\mu^2\sum_{x=0}^{\infty}x^2\left[\left(1-\theta^{1/x}\right)^{\beta}-\left(1-\theta^{1/(x+1)}\right)^{\beta}\right]-3\mu^4\right\}.\end{aligned} \tag{16}$$

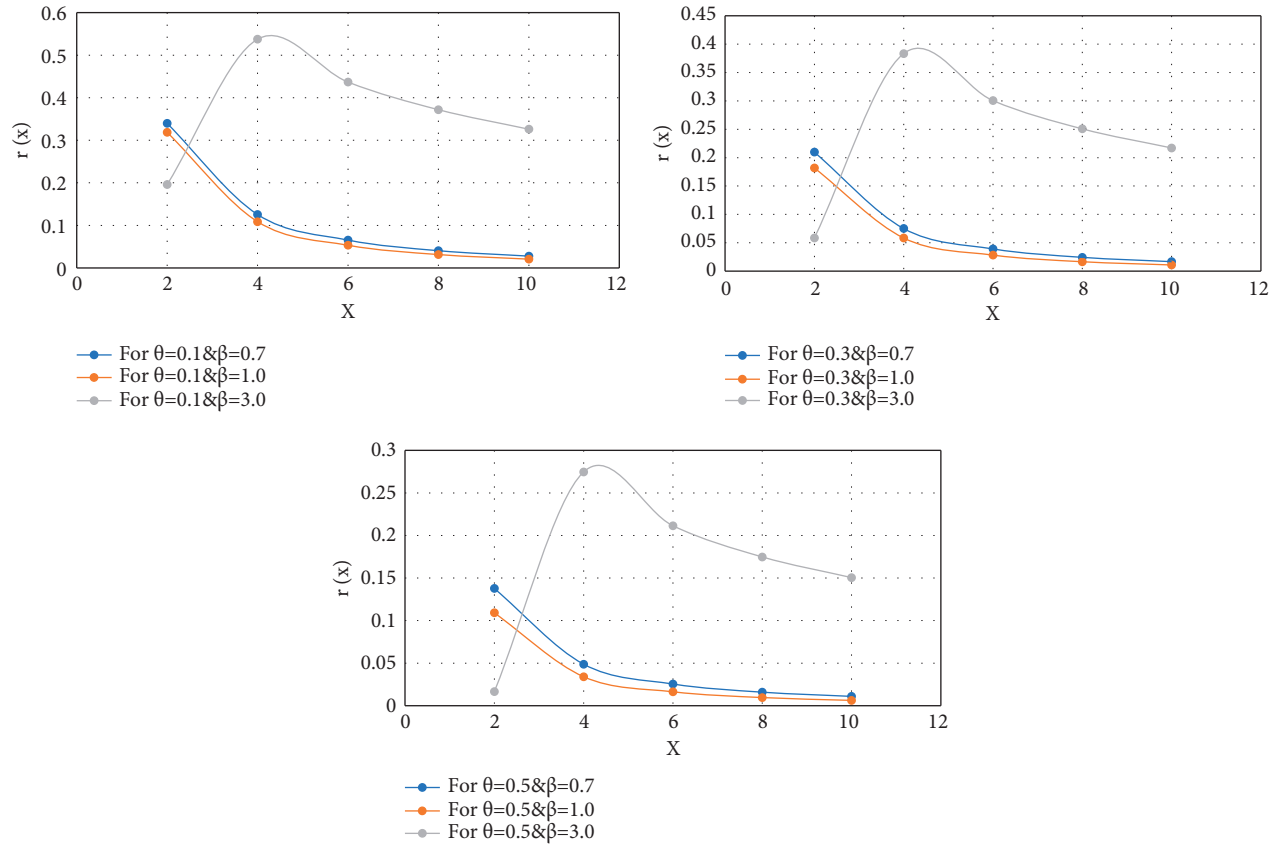

Figure 3: RHRF of the **DGIE**(β, θ).

The probability generating function (PGF), $G(t)$, of DGIE(β, θ) distribution is obtained as follows:

$$G(t) = E[t^x] = \sum_{x=0}^{\infty} t^x P(X = x) = \sum_{x=0}^{\infty} t^x \left[\left(1 - \theta^{1/x}\right)^{\beta} - \left(1 - \theta^{1/(x+1)}\right)^{\beta}\right]. \tag{17}$$

For simplicity, we compute the PGF numerically where the rth the factorial moment is computed as

$$\mu_{[r]} = G^r(1) = \frac{\alpha}{\alpha - 1} \sum_{x=0}^{\infty} x(x-1) \ldots\ldots\ldots\ldots (x - r + 1)\left[\left(1 - \theta^{1/x}\right)^{\beta} - \left(1 - \theta^{1/(x+1)}\right)^{\beta}\right]. \tag{18}$$

The variance, the variance (σ^2) of DGIE(β, θ) distribution is given by the following:

$$\begin{aligned} \operatorname{var}(X) = \sigma^2 &= G''(1) + G^{\cdot}(1) - \left(G^{\cdot}(1)\right)^2 \\ &= \frac{\alpha}{\alpha - 1} \sum_{x=0}^{\infty} x^2 \left[\left(1 - \theta^{1/x}\right)^{\beta} - \left(1 - \theta^{1/(x+1)}\right)^{\beta}\right] - \left(\frac{\alpha}{\alpha - 1} \sum_{x=0}^{\infty} x\left[\left(1 - \theta^{1/x}\right)^{\beta} - \left(1 - \theta^{1/(x+1)}\right)^{\beta}\right]\right)^2. \end{aligned} \tag{19}$$

Characteristic function: the characteristic function (CF), $\phi_X(w)$ of DGIE(β, θ) distribution is of the form:

$$\phi_X(w) = E\left[e^{iwx}\right] = \sum_{x=0}^{\infty} e^{iwx} P(X = x) = \frac{\alpha}{\alpha - 1} \sum_{x=0}^{\infty} e^{iwx} \left[\left(1 - \theta^{1/x}\right)^{\beta} - \left(1 - \theta^{1/(x+1)}\right)^{\beta}\right]. \tag{20}$$

Because moments do not have closed forms, the mean and variance can only be calculated numerically. We estimated mean and variance for various values of β and θ in Tables 1 and 2, respectively.

2.3. Order Statistics. Order statistics has a deep reflection on theoretical and practical aspects of statistics. This importance is shown in statistical inference and nonparametric statistics. Let $X_1, X_2, \ldots.., X_n$ be a random sample from A DGIE(β, θ) distribution, and let $X_{1:n}, X_{2:n}, \ldots.., X_{n:n}$ be the order statistics. Then, the CDF of the i^{th} order statistics for x can be represented in the for

$$\begin{aligned} F_{i:n}(x, \alpha, \theta) &= \sum_{k=i}^{n} \binom{n}{k} [F_i(x, \beta, \theta)]^k [F_i(x, \beta, \theta)] a \\ &= \sum_{k=i}^{n} \sum_{m=0}^{\beta k} (-1)^m \binom{n}{k} \binom{\beta k}{m} \theta^{m\beta/(x+1)} \left[\left(1 - \theta^{1/(x+1)}\right)^{\beta}\right]^{n+m-k}. \end{aligned} \tag{21}$$

Therefore, the PMF of the k^{th} Os has the form:

$$f_{k:n}(x, \alpha, \theta, \beta) = \sum_{m=0}^{k-1} \Theta_m^{(n,\beta(k-1))} \theta^{m/(x+1)} \left[\left(1 - \theta^{(x+1)}\right)^{\beta}\right]^{n+m-k} \left[\left(1 - \theta^{1/x}\right)^{\beta} - \left(1 - \theta^{1/(x+1)}\right)^{\beta}\right], \tag{22}$$

where $\Theta_m^{(n,k-1)} = (-1)^m \binom{\beta k}{m} n!/(k-1)!(n-k)!$.

So, the q^{th} moments of $X_{i:n}$ is written in the form:

$$E\left[X_{i:n}^q\right] = \sum_{x=0}^{\infty} \sum_{m=0}^{k-1} \Theta_m^{(n,\beta(k-1))} \theta^{m/(x+1)} x^q \left[\left(1 - \theta^{(x+1)}\right)^{\beta}\right]^{n+m-k} \left[\left(1 - \theta^{1/x}\right)^{\beta} - \left(1 - \theta^{1/(x+1)}\right)^{\beta}\right], \tag{23}$$

where $\Theta_m^{(n,k-1)} = (-1)^m \binom{\beta k}{m} n!/(k-1)!(n-k)!$.

2.3.1. Renyi Entropy. Renyi entropy plays a vital role in information theory. The Renyi entropy of a random variable X is defined as:

$$I_R(\gamma) = \frac{1}{1 - \gamma} \log \sum_x (P(X = x))^{\gamma}, \tag{24}$$

where $\gamma > 0$ and $\gamma \neq 1$ (Renyi, 1961). For the DGIE(β, θ)) distribution for γ is an integer number, we compute

$$\sum_{x=0}^{\infty} (P(X = x))^{\gamma} = \sum_{j=0}^{\gamma} \left[\left(1 - \theta^{1/j}\right)^{\beta} - \left(1 - \theta^{1/j+1}\right)^{\beta}\right]^{\gamma} I_R(\gamma) = \frac{1}{1 - \gamma} \log \sum_{j=0}^{\gamma} \left[\left(1 - \theta^{1/j}\right)^{\beta} - \left(1 - \theta^{1/(j+1)}\right)^{\beta}\right]^{\gamma}. \tag{25}$$

2.4. Unknown Parameters Estimation. In this section, we used two methods to estimate DGIE(β, θ) distribution unknown parameters using

2.4.1. Maximum Likelihood Method. Let $X_1, X_2, \ldots.., X_n$ represents the lifetimes of n independent test units which

Following DGIE(β, θ). So, its log-likelihood function is written as: $p(x) = (1 - \theta^{1/x})^{\beta} - (1 - \theta^{1/(x+1)})^{\beta}$

Table 1: The mean of the DGIE(β, θ) distribution.

β/θ	0.1	0.2	0.3	0.4	0.5	0.6	0.7	0.8
2	2.682	1.711	1.153	0.774	0.502	0.304	0.163	0.069
3	1.471	0.861	0.522	0.307	0.169	0.083	0.034	0.009
4	1.043	0.559	0.303	0.156	0.072	0.029	0.009	0.001
5	0.814	0.398	0.193	0.086	0.033	0.010	0.0025	0.0003

Table 2: The variance of the **DGIE**(β, θ) distribution.

β/θ	0.1	0.2	0.3	0.4	0.5	0.6	0.7	0.8
3	6.317	2.822	1.449	0.7621	0.385	0.177	0.068	0.018
4	2.371	0.997	0.481	0.232	0.103	0.039	0.012	0.002
5	1.300	0.526	0.239	0.104	0.040	0.012	0.002	0.0003
6	0.845	0.334	0.141	0.054	0.017	0.004	0.001	0.001

$$L[P(X=x)] = \prod_{i=1}^{n} p(x_i) = \prod_{i=1}^{n} \left(1-\theta^{1/x_i}\right)^{\beta} - \left(1-\theta^{1/(x_i+1)}\right)^{\beta},$$
$$I(x, \alpha, \theta) = \sum_{i=1}^{n} \ln\left(\left(1-\theta^{1/x_i}\right)^{\beta} - \left(1-\theta^{1/(x_i+1)}\right)^{\beta}\right). \tag{26}$$

Likelihood equations are then obtained as follows:

$$\frac{\delta l}{\delta \theta} = \sum_{i=1}^{n} \frac{-1/x_i - 1\beta\theta^{1/x_i - 1}\left(1-\theta 1/x_i\right)^{\beta} + \beta 1/(x_i+1)\left(1-\theta^{1/(x_i+1)}\right)^{\beta-1}\theta^{1/(x_i+1)}}{\left(1-\theta^{1/x_i}\right)^{\beta} - \left(1-\theta^{1/(x_i+1)}\right)^{\beta}} = 0,$$
$$\frac{\delta l}{\delta \beta} = \sum_{i=0}^{n} \frac{\left(1-\theta^{1/x_i}\right)^{\beta} \ln\left(1-\theta^{1/x_i}\right)^{\beta} - \left(1-\theta^{1/(x_i+1)}\right)^{\beta} \ln\left(1-\theta^{1/(x_i+1)}\right)}{\left(1-\theta^{1/x_i}\right)^{\beta} - \left(1-\theta^{1/(x_i+1)}\right)^{\beta}} = 0. \tag{27}$$

We can obtain the solution of these equations numerically then; we compute the Fisher's information matrix by finding the second partial derivatives

$$I_x(\beta, \theta) = \begin{bmatrix} -E\left[\dfrac{\partial^2 l}{\partial \beta^2}\right] & -E\left[\dfrac{\partial^2 l}{\partial \beta\, \partial \theta}\right] \\ -E\left[\dfrac{\partial^2 l}{\partial \theta\, \partial \beta}\right] & -E\left[\dfrac{\partial^2 l}{\partial \theta^2}\right] \end{bmatrix}. \tag{28}$$

One can infer that the DGIE(β, θ) distribution satisfies the regularity conditions [23]. Then, the MLE vector $(\widehat{\beta}, \widehat{\theta})^T$ is asymptotically normal and consistent. Fisher's information matrix can be approximated as

$$I_x(\alpha, \theta) = \begin{bmatrix} -\dfrac{\partial^2 l}{\partial \beta^2}\Big|_{(\widehat{\beta},\widehat{\theta})} & -\dfrac{\partial^2 l}{\partial \beta\, \partial \theta}\Big|_{(\widehat{\beta},\widehat{\theta})} \\ -\dfrac{\partial^2 l}{\partial \theta\, \partial \beta}\Big|_{(\widehat{\beta},\widehat{\theta})} & -\dfrac{\partial^2 l}{\partial \theta^2}\Big|_{(\widehat{\beta},\widehat{\theta})} \end{bmatrix}, \tag{29}$$

where $\widehat{\beta}$ and $\widehat{\theta}$ are the MLEs of β and θ [24].

The element of the hessian matrix $I_x(\alpha, \theta)$ are obtained from

$$\frac{\partial^2 l}{\partial \beta^2} = \sum_{i=0}^{n} \frac{\left[\left(1-\theta^{1/x_i}\right)^{\beta} - \left(1-\theta^{1/(x_i+1)}\right)^{\beta}\right]\left[\left(1-\theta^{1/x_i}\right)^{\beta}\left(\ln\left(1-\theta^{1/x_i}\right)\right)^2 - \left(1-\theta^{1/(x_i+1)}\right)^{\beta}\left(\ln\left(1-\theta^{1/(x_i+1)}\right)\right)^2\right.}{\left(\left(1-\theta^{1/x_i}\right)^{\beta} - \left(1-\theta^{1/(x_i+1)}\right)^{\beta}\right)^2} a$$

$$- \frac{\left[\left(1-\theta^{1/x_i}\right)^{\beta}\ln\left(1-\theta^{1/x_i}\right) - \left(1-\theta^{1/(x_i+1)}\right)^{\beta}\ln\left(1-\theta^{1/(x_i+1)}\right)\right]\left[\left(1-\theta^{1/x_i}\right)^{\beta}\ln\left(1-\theta^{1/x_i}\right) - \left(1-\theta^{1/(x_i+1)}\right)^{\beta}\ln\left(1-\theta^{1/(x_i+1)}\right)\right.}{\left(\left(1-\theta^{1/x_i}\right)^{\beta} - \left(1-\theta^{1/(x_i+1)}\right)^{\beta}\right)^2}$$

$$\frac{\partial^2 l}{\partial \theta\, \partial \beta} = \sum_{i=0}^{n} \frac{\left[\left(1-\theta^{1/x_i}\right)^{\beta} - \left(1-\theta^{1/(x_i+1)}\right)^{\beta}\right]\left[-1/x_i\theta^{1/x_i}\left(1-\theta^{1/x_i}\right)^{\beta} - 1/x_i\beta\theta^{1/x_i-1}\left(1-\theta^{1/x_i}\right)^{\beta}\ln\left(1-\theta^{1/x_i}\right)\right.}{\left(\left(1-\theta^{1/x_i}\right)^{\beta} - \left(1-\theta^{1/(x_i+1)}\right)^{\beta}\right)^2}$$

$$+ \frac{1/(x_i+1)\theta^{1/x_i+1}\left(1-\theta^{1/(x_i+1)}\right)^{\beta-1} + \beta 1/(x_i+1)\theta^{1/x_i+1}\left(1-\theta^{1/(x_i+1)}\right)^{\beta-1}\ln\left(1-\theta^{1/(x_i+1)}\right)}{\left(\left(1-\theta^{1/x_i}\right)^{\beta} - \left(1-\theta^{1/(x_i+1)}\right)^{\beta}\right)^2}$$

$$- \frac{\left(-1/x_i\beta\theta^{1/x_i-1}\left(1-\theta^{1/x_i}\right)^{\beta} + \beta 1/(x_i+1)\theta^{1/x_i+1}\left(1-\theta^{1/(x_i+1)}\right)^{\beta-1}\right)\left(\left(1-\theta^{1/x_i}\right)^{\beta}\ln\left(1-\theta^{1/x_i}\right) - \left(1-\theta^{1/(x_i+1)}\right)^{\beta}\ln\left(1-\theta^{1/(x_i+1)}\right)\right)}{\left(\left(1-\theta^{1/x_i}\right)^{\beta} - \left(1-\theta^{1/(x_i+1)}\right)^{\beta}\right)^2}$$

$$\frac{\partial^2 l}{\partial \theta^2} = \sum_{i=0}^{n} \frac{\left[\left(1-\theta^{1/x_i}\right)^{\beta} - \left(1-\theta^{1/(x_i+1)}\right)^{\beta}\right]\left[-\beta 1/x_i(1/x_i-1)\theta^{1/x_i-2}\left(1-\theta^{1/x_i}\right)^{\beta} + 1/x_i^2\beta^2\theta^{2(1/x_i-1)}\left(1-\theta^{1/x_i}\right)^{\beta}\right.}{\left(\left(1-\theta^{1/x_i}\right)^{\beta} - \left(1-\theta^{1/(x_i+1)}\right)^{\beta}\right)^2}$$

$$+ \frac{\beta 1/(x_i+1)^2\theta^{1/x_i-1-1}\left(1-\theta^{1/(x_i+1)}\right)^{\beta-1} + \beta(\beta-1)1/(x_i+1)^2\theta^{1/x_i-1-1}\left(1-\theta^{1/(x_i+1)}\right)^{\beta-2}}{\left(\left(1-\theta^{1/x_i}\right)^{\beta} - \left(1-\theta^{1/(x_i+1)}\right)^{\beta}\right)^2}$$

$$- \frac{\left(-1/x_i\beta\theta^{1/x_i-1}\left(1-\theta^{1/x_i}\right)^{\beta} + \beta 1/(x_i+1)\theta^{1/x_i-1}\left(1-\theta^{1/(x_i+1)}\right)^{\beta-1}\right) - \left(\beta 1/x_i\left(1-\theta^{1/x_i-1}\right)^{\beta-1} + \beta 1/(x_i+1)\left(1-\theta^{1/(x_i+1)}\right)^{\beta-1}\right.}{\left(\left(1-\theta^{1/x_i}\right)^{\beta} - \left(1-\theta^{1/(x_i+1)}\right)^{\beta}\right)^2}. \tag{30}$$

2.4.2. Method of Moments Estimation. We can find moments' estimates (MM E_s) of (β, θ) by solving the equations

$$\begin{aligned} \sum_{i=1}^{\infty} x_i\left[\left(1-\theta^{1/x_i}\right)^{\beta} - \left(1-\theta^{1/(x_i+1)}\right)^{\beta}\right] &= \mu_1^{[1]}, \\ \sum_{i=1}^{\infty} x_i^2\left[\left(1-\theta^{1/x_i}\right)^{\beta} - \left(1-\theta^{1/(x_i+1)}\right)^{\beta}\right] &= \mu_2^{[2]}, \end{aligned} \tag{31}$$

where $\mu_1^{[1]}$ and $\mu_2^{[2]}$ represent the first and the second sample moments.

3. Results and Discussion

3.1. A Simulation Study. In this section, we assess the performance of the maximum-likelihood estimate with respect to sample size n. The assessment is based on a simulation study:

(1) Generate 10000 samples of size n from equation (1). The inversion method is used to generate samples; that is, varieties of the discrete generalized inverted exponential distribution are generated using

$$X = \frac{\ln \theta}{\ln\left(1 - (1 - u)^{1/\beta}\right)} - 1; 0 < u < 1, \tag{32}$$

where $U \sim U(0, 1)$ is a uniform variable on the unit interval.

(2) Compute the Maximum-likelihood Estimates for 10000 Samples, Say $\widehat{\theta}_{\mathbf{i}}$ for

$$i = 1, 2, \ldots, 10000. \tag{33}$$

(3) Compute the biases and mean-squared errors given by

$$\begin{aligned} \text{bias}(n) &= \frac{1}{10000} \sum_{i=1}^{10000} \left(\widehat{\theta}_i - \theta_i\right), \\ \text{MSE}(n) &= \frac{1}{10000} \sum_{i=1}^{10000} \left(\widehat{\theta}_i - \theta_i\right)^2. \end{aligned} \tag{34}$$

The empirical results are given in Table 3. From Table 3, the following observations can be noted: the magnitude of the bias always decreases to zero as $\mathbf{n} \longrightarrow \infty$. The MSEs always decrease to zero as $\mathbf{n} \longrightarrow \infty$. This shows the consistency of the estimators.

3.1.1. Data Application. We pointed out here, the notability of a discrete generalized inverted exponential distribution on distributions: geometric distribution, discrete logistic distribution and discrete Lindley distribution. Two real data sets are applied. The first data are in Table 4 is for 30 failure times of the air conditioning system of an airplane. These data are taken from [25].

The MLE of (β, θ) values in all these cases has been computed. The Kolmogorov–Smirnov (K–S) measure in each case and the associated P value are computed. The result is put in Table 5.

The Akaike information criterion (AIC), correct Akaike information criterion (CAIC) and Bayesian Akaike information criterion (BIC) values for the models have been computed. The result is reported in Table 6. The Akaike's measures indicate that the GIED distribution fits the data better than some existing distributions for this data set.

The data set given in Table 7 consists of uncensored data from [23]. The data gives 100 observations on breaking stress of carbon fibers (in Gba). The MLE of (β, θ) values in all these cases have been computed. The Kolmogorov–Smirnov (K-S) measure in each case and the associated p-value are computed. The result is put in Table 8. A comparison between the observed and the fitted distributions are shown in Figures 4 and 5.

The Akaike's measures indicate that the GIED distribution fits the data better than some existing distributions for this data set, as in Table 9. For the first, second data sets, the discrete generalized inverted exponential distribution shows the best convenient p values. The distribution plots propose that the discrete generalized inverted exponential distribution offers the best fit between the competitor distributions. On the basis of the tabulated results, we infer that the discrete generalized inverted exponential distribution provides the best fit compared to its submodels. Some summary statistics of data sets 1 and 2 are listed in Table 10.

3.2. Image Segmentation. In this section, we assess the ability of DGIED to improve the performance of segmentation the image. This can be performed by considering it as a clustering method.

3.2.1. Clustering Problem Formulation for Image Segmentation. In this part, we introduce the mathematical formulation of the automatic clustering-based image segmentation problem. In general, the main aim of AC is to split the given image $\mathbf{I}$ into a set of $K_{\max}$ groups. To perform this task, the between-cluster variation must be maximized at the same time with minizing within-cluster variation.

Therefore, the mathematical representation of AC can be given by dividing the image into $K_{\max}$ cluster (i.e., $\mathbf{C}_1, \mathbf{C}_2, \ldots, \mathbf{C}_{\mathbf{K}_{\max}}$) with satisfied the following criteria:

$$\begin{aligned} &\cup_{\mathbf{l}=1}^{\mathbf{K}_{\max}} \mathbf{C}_{\mathbf{l}} = \mathbf{I}, \mathbf{C}_{\mathbf{l}} \neq \phi, \ \mathbf{l} = 1, \ldots, \mathbf{K}_{\max} \\ &\mathbf{C}_{\mathbf{l}} \cap \mathbf{C}_{\mathbf{l}1} = \phi, \mathbf{l}, \mathbf{l}1 = 1, 2, \ldots, \mathbf{K}_{\max}, \mathbf{l} \neq \mathbf{l}1. \end{aligned} \tag{35}$$

Gaussian mixture models (GMM): it is one of the most popular clustering techniques, and it has been used as an image segmentation method in different applications, for example, image retrieval [26], chemical and physical properties of Italian wines, and the chemical [27, 28] and others [29].

The mathematical formulation of the Gaussian mixture model (GMM) can be represented by considering the given image $\mathbf{I}$ consisting of a set of pixels $\mathbf{X}$ that are represented as a random variable. So, the GMM can be defined as

$$f(x) = \sum_{i=1}^{K} w_i N\left(x|\mu_i, \sigma_i^2\right). \tag{36}$$

In equation (36), K represents the number of objects and $w_i > 0$ refer to the weights where $\sum_{i=1}^{K} w_i = 1$. In addition, the $N(x|\mu_i, \sigma_i^2)$ is defined as

$$N\left(x|\mu_i, \sigma_i^2\right) = \frac{1}{\sigma\sqrt{2\pi}} e^{-\left(x-\mu_i\right)^2/2\sigma_i^2}, \tag{37}$$

Table 3: The averages bias and averages MSE for simulated results of ML estimates.

	$\beta = 0.779$					
Sample size	$\theta = 8.763 * 10^{-6}$		$\theta = 1.671 * 10^{-5}$		$\theta = 2.823 * 10^{-6}$	
	Bias	MSE	Bias	MSE	Bias	MSE
10	$-4.064 * 10^{-5}\,(4.224 * 10^{-5})$	$1.651 * 10^{-9}\,(1.785 * 10^{-9})$	$-0.05\,(1.178 * 10^{-4})$	$2.486 * 10^{-3}\,(1.388 * 10^{-8})$	$-3.541 * 10^{-8}\,(1.504 * 10^{-5})$	$1.254 * 10^{-15}\,(2.263 * 10^{-10})$
70	$-6.59 * 10^{-10}\,(9.092 * 10^{-7})$	$0\,(8.266 * 10^{-13})$	$-0.017\,(5.958 * 10^{-6})$	$2.933 * 10^{-4}\,(3.55 * 10^{-11})$	$-3.788 * 10^{-12}\,(8.225 * 10^{-8})$	$0\,(6.765 * 10^{-15})$
130	$3.139 * 10^{-10}\,(-3.257 * 10^{-7})$	$0\,(1.061 * 10^{-13})$	$0.041\,(-5.469 * 10^{-6})$	$1.656 * 10^{-3}\,(2.991 * 10^{-11})$	$4.173 * 10^{-11}\,(-1.977 * 10^{-7})$	$0\,(3.91 * 10^{-14})$
210	$-9.771 * 10^{-9}\,(1.728 * 10^{-5})$	$0\,(2.987 * 10^{-10})$	$0.039\,(1.812 * 10^{-5})$	$1.499 * 10^{-3}\,(3.285 * 10^{-10})$	$2.595 * 10^{-10}\,(5.774 * 10^{-6})$	$0\,(3.334 * 10^{-11})$
	$\theta = 8.763 * 10^{-6}$					
Sample size	$\beta = 1.2$		$\beta = 26.715$		$\beta = 0.779$	
	Bias	MSE	Bias	MSE	Bias	MSE
10	$-2.274 * 10^{-4}\,(5.067 * 10^{-5})$	$5.172 * 10^{-8}\,(2.568 * 10^{-9})$	$-17.327\,(1.392 * 10^{-3})$	$3.232 * 10^{-14}\,(1.937 * 10^{-6})$	$-4.064 * 10^{-5}\,(4.224 * 10^{-5})$	$1.651 * 10^{-9}\,(1.785 * 10^{-9})$
70	$-5.551 * 10^{-10}\,(3.192 * 10^{-6})$	$0\,(1.019 * 10^{-11})$	$-6.203 * 10^{-7}\,(3.765 * 10^{-5})$	$3.847 * 10^{-13}\,(1.418 * 10^{-9})$	$-5.793 * 10^{-10}\,(1.017 * 10^{-6})$	$0\,(1.034 * 10^{-12})$
130	$4.006 * 10^{-10}\,(1.893 * 10^{-6})$	$0\,(3.584 * 10^{-12})$	$-5.778 * 10^{-7}\,(4.017 * 10^{-5})$	$3.338 * 10^{-13}\,(1.613 * 10^{-9})$	$3.436 * 10^{-10}\,(-2.201 * 10^{-7})$	$0\,(4.844 * 10^{-14})$
210	$-2.831 * 10^{-8}\,(1.876 * 10^{-5})$	$0\,(3.518 * 10^{-10})$	$-6.466 * 10^{-7}\,(5.427 * 10^{-5})$	$4.181 * 10^{-13}\,(2.945 * 10^{-9})$	$-1.065 * 10^{-8}\,(1.735 * 10^{-5})$	$0\,(3.011 * 10^{-10})$

Table 4: Data set 1.

23	62	42	3	16
261	47	20	14	90
87	225	5	71	1
7	71	12	11	16
120	246	120	14	52
14	21	11	11	95

Table 5: The results of data set 1.

Distribution	$p(x)$	Estimates of parameters	p value	K-S statistics
Discrete generalized inverted exponential distribution	(2.2)	$\theta = 8.763 \times 10^{-6}$ $\beta = 0.779$	$0.237755 * 10^{-2}$	0.326379
Geometric	$p(1-p)^x$	$p = 0.017$	$0.5382 * 10^{-5}$	0.45039
Discrete logistic	$(1-p)p^{x-\mu}/(1+p^{x-\mu})(1+p^{x-\mu+1})$	$p = 0.083$, $\mu = -30.999$	6.968×10^{-28}	1
Discrete lindley	$\lambda^x/1 - \log\lambda[\lambda \log\lambda + (1-\lambda)(1-\log\lambda^{x+1})]$	$\lambda = 0.401$	1.198124×10^{-10}	0.610163

Table 6: AIC, CAIC and BIC measures for data set 1.

	Distribution	AIC	CAIC	BIC
$N = 30$	DGIE	312.880	313.324	315.683
	Geometric	314.397	314.539	315.798
	Discrete lindely	478.532	478.673	479.9314
	Discrete logistic	13628.219	13628.659	13631.017

Table 7: Data set 2.

3.7	2.74	2.73	2.5	3.6
3.11	3.27	2.87	1.47	3.11
4.42	2.41	3.19	3.22	1.69
3.28	3.09	1.87	3.15	4.9
3.75	2.43	2.95	2.97	3.39
2.96	2.53	2.67	2.93	3.22
3.39	2.81	4.2	3.33	2.55
3.31	3.31	2.85	2.56	3.56
3.15	2.35	2.55	2.59	2.38
2.81	2.77	2.17	2.83	1.92
1.41	3.68	2.97	1.36	0.98
2.76	4.91	3.68	1.84	1.59
3.19	1.57	0.81	5.56	1.73
1.59	2	1.22	1.12	1.71
2.17	1.17	5.08	2.48	1.18
3.51	2.17	1.69	1.25	4.38
1.84	0.39	3.68	2.48	0.85
1.61	2.79	4.7	2.03	1.8
1.57	1.08	2.03	1.61	2.12
1.89	2.88	2.82	2.05	3.65

Table 8: The results of data set 2.

Distribution	$p(x)$	Estimates of parameters	p value	K-S statistics
Discrete generalized inverted exponential distribution	(2.2)	$\theta = 1.671 \times 10^{-5}\beta = 26.715$	$2.19 * 10^{-7}$	0.279787
Geometric	$p(1-p)^x$	$p = 0.381$	$1.653 * 10^{-31}$	0.591263
Discrete logistic	$(1-p)p^{x-\mu}/(1+p^{x-\mu})(1+p^{x-\mu+1})$	$p = 0.132$, $\mu = -38.28$	2.45×10^{-89}	1
Discrete lindley	$\lambda^x/1 - \log\lambda[\lambda\log\lambda + (1-\lambda)(1-\log\lambda^{x+1})]$	$\lambda = 0.599$	8.6704×10^{-13}	0.372892

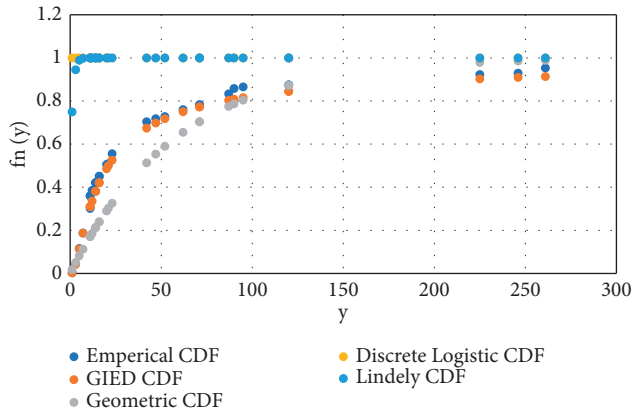

Figure 4: Distribution plots for data set 1.

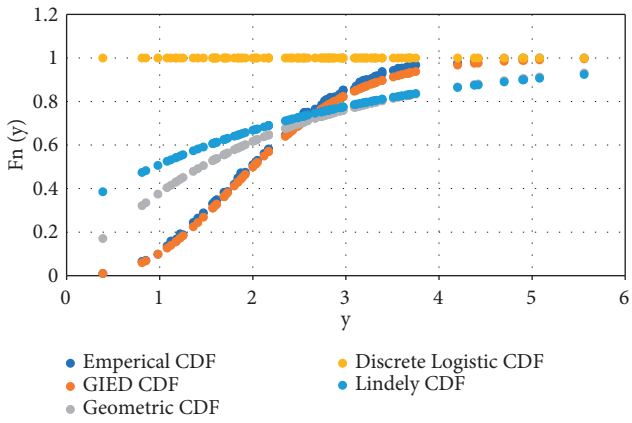

Figure 5: Distribution plots for data set 2.

Table 9: AIC, CAIC and BIC measures for data set 2.

	Distribution	AIC	CAIC	BIC
$N = 100$	DGIE	314.445	314.569	319.655
	Geometric	400.411	400.541	403.016
	Discrete lindely	422.027	422.067	424.632
	Discrete logistic	16832.972	16833.095	16838.182

where μ_i and σ_i are mean and the standard deviation of class $\mathbf{i}$. For image $\mathbf{X}$, the parameters are $\theta = (\mathbf{w}_1, \ldots, \mathbf{w}_k, \mu_1, \ldots, \mu_k, \sigma_1^2, \ldots, \sigma_k^2)$ are required to determine and to achieve this estimation, the Expectation-Maximization (EM) method is used. The steps of EM can be summarized as in Algorithm 1:

However, the traditional GMM has some limitations that influence its performance, such as inefficiency in modeling all the data types, including discrete data in the application such as machine learning [30]. To avoid these limitations, we use the new distribution named Discrete Generalized Inverted Exponential Distribution. In general, DGIED has the ability to tackle the non-inaccurateness of using general distributions such as mixture Gaussian distribution.

3.2.2. Dataset Description. In this study, the performance of the developed clustering-based color image segmentation using DGIED mixture model (DGIEMM) is evaluated using a set of six color images (as in Figures 6(a)–6(f)) [31]. In addition, we compared the results of DGIEMM with GMM, K-means, and Fuzzy subspace clustering (FSC).

3.2.3. Performance Measures. To evaluate the efficacy of the developed image segmentation, a set of performance measures is used. For example, Accuracy, Adjust Rand Index, Hubert, and Normalized mutual information. The details of these measures are given as follows:

Accuracy: It is a measure used to assess the ability of the method to determine the optimal cluster for each pixel. It is formulated as

$$\text{accuracy} = \frac{\text{TP} + \text{TN}}{\text{TP} + \text{FP} + \text{TN} + \text{FN}}, \tag{38}$$

where TP, FP, TN, and FN are the True positive, False positive, True negative, and False negative.

Adjust Rand Index: It is a measure used to assess the similarity between two groups, and it is defined as:

$$\mathbf{ARI} = \frac{\sum_{ij}\binom{\mathbf{n}_{ij}}{2} - \left[\sum_i \binom{\mathbf{a}_i}{2}\sum_j \binom{\mathbf{b}_j}{2}\right] / \binom{\mathbf{n}}{2}}{0.5\left[\sum_i \binom{\mathbf{a}_i}{2} + \sum\sum_j \binom{\mathbf{b}_j}{2}\right] - \left[\sum_i \binom{\mathbf{a}_i}{2}\sum_j \binom{\mathbf{b}_j}{2}\right] / \binom{\mathbf{n}}{2}}, \tag{39}$$

Table 10: Some statistical measures for data sets.

Data set	Mean	Median	Std. deviation	Variance	Skewness	Kurtosis	Minimum	Maximum
I	28.73429	22	70.67654	5167.421	1.784077	2.568813	1	261
II	2.404559	2.7	1.008803	1.027964	0.373784	0.172868	0.39	5.56

(1) Input: image $\mathbf{X_j}$, $\mathbf{j} = 1, \ldots, \mathbf{n}$ and $\mathbf{i} \in \{1, 2, \ldots, \mathbf{k}\}$ are the label set $\mathbf{Y} = \{\mathbf{y_1}, \mathbf{y_2}, \ldots, \mathbf{y_N}\}, \mathbf{y_n} \in \{1, \ldots, \mathbf{K}\}$
(2) Initialize $\theta^0 = (\mathbf{p_1^0}, \ldots, \mathbf{p_k^0}, \mu_1^0, \ldots, \mu_k^0, \sigma_1^{2(0)}, \ldots, \sigma_k^{2(0)})$:
(3) While (condition not met)
(4) E-Step:

$$\mathbf{p_{ij}^{r+1}} = \mathbf{p_{ij}^{r+1}}(\mathbf{i}|\mathbf{x_j}) = \mathbf{w_i^r N}(\mathbf{x_j}|\mu_i^{(r)}, \sigma_i^{2(r)})/\mathbf{f}(\mathbf{x_j})$$

(5) M-Step

$$\widehat{\mathbf{w}}_{\mathbf{ij}}^{\mathbf{r+1}} = 1/\mathbf{n} \sum_{\mathbf{j=1}}^{\mathbf{n}} \mathbf{w_{ij}^r}$$

$$\widehat{\mu}_{\mathbf{ij}}^{\mathbf{r+1}} = \sum_{\mathbf{j=1}}^{\mathbf{n}} \mathbf{w_{ij}^{r+1}} \mathbf{x_j}/\mathbf{n}\widehat{\mathbf{w}}_{\mathbf{ij}}^{\mathbf{r+1}}$$

$$\widehat{\sigma}_{\mathbf{i}}^{2(\mathbf{r+1})} = \sum_{\mathbf{j=1}}^{\mathbf{n}} \mathbf{w_{ij}^{r+1}} (\mathbf{x_j} - \widehat{\mu}_{\mathbf{i}}^{\mathbf{r+1}})/\mathbf{n})$$

End While
(6) For each data vector $\mathbf{x_n}$, set.

$$\mathbf{y_n} = \arg\max_{\mathbf{i}} (\mathbf{w_i N}(\mathbf{x}|\mu_\mathbf{i}, \sigma_\mathbf{i}^2))$$

Algorithm 1: Steps of EM method.

I1

(a)

I2

(b)

I3

(c)

I4

(d)

Figure 6: Continued.

I5

(e)

I6

(f)

Figure 6: The original tested images used in this study. (a) I1, (b) I2, (c) I3, (d) I4, (e) I5, (f) I6.

Table 11: Comparison between developed method and other segmentation methods.

		DGIEMM	FSC	GMM	K-means		DGIEMM	FSC	GMM	K-means
I1	Accuracy	0.9951	0.9494	0.6259	0.6259	I4	0.9886	0.9086	0.9013	0.9515
	AR	0.9803	0.8068	0.9572	0.9134		0.9548	0.6679	0.6441	0.7422
	Hubert	0.9805	0.8078	0.8634	0.8886		0.9548	0.6679	0.6442	0.7141
	NMI	0.9574	0.7474	0.8373	0.8726		0.9208	0.6419	0.5919	0.6986
I2	Accuracy	0.9995	0.9880	0.8956	0.8956	I5	0.9998	0.9964	0.9899	0.5614
	AR	0.9978	0.9510	0.6224	0.6224		0.9993	0.9858	0.9600	0.0785
	Hubert	0.9979	0.9526	0.6260	0.6260		0.9993	0.9858	0.9601	0.0543
	NMI	0.9931	0.9076	0.5820	0.5820		0.9978	0.9691	0.9276	0.1884
I3	Accuracy	0.9913	0.9867	0.9280	0.9274	I6	0.9982	0.9928	0.8972	0.9198
	AR	0.9647	0.9468	0.7227	0.7206		0.9915	0.9666	0.6047	0.6251
	Hubert	0.9653	0.9476	0.7326	0.7306		0.9928	0.9716	0.6311	0.7240
	NMI	0.9306	0.8926	0.6554	0.6537		0.9762	0.9160	0.5463	0.6547

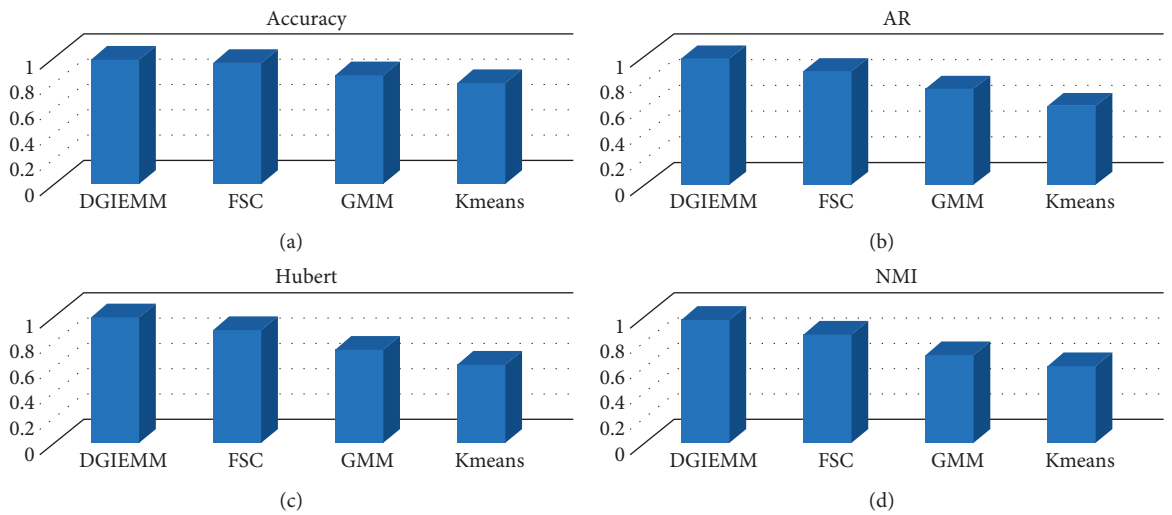

Figure 7: Average of each method in terms of (a) accuracy, (b) AR, (c) Hubert, and (d) NMI.

Table 12: Mean-rank obtained by each algorithm.

	DGIEMM	FSC	GMM	K-means
Accuracy	4	2.8333	1.5000	1.6667
AR	4	2.5000	1.7500	1.7500
Hubert	4	2.5000	1.5833	1.9167
NMI	4	2.5000	1.5833	1.9167

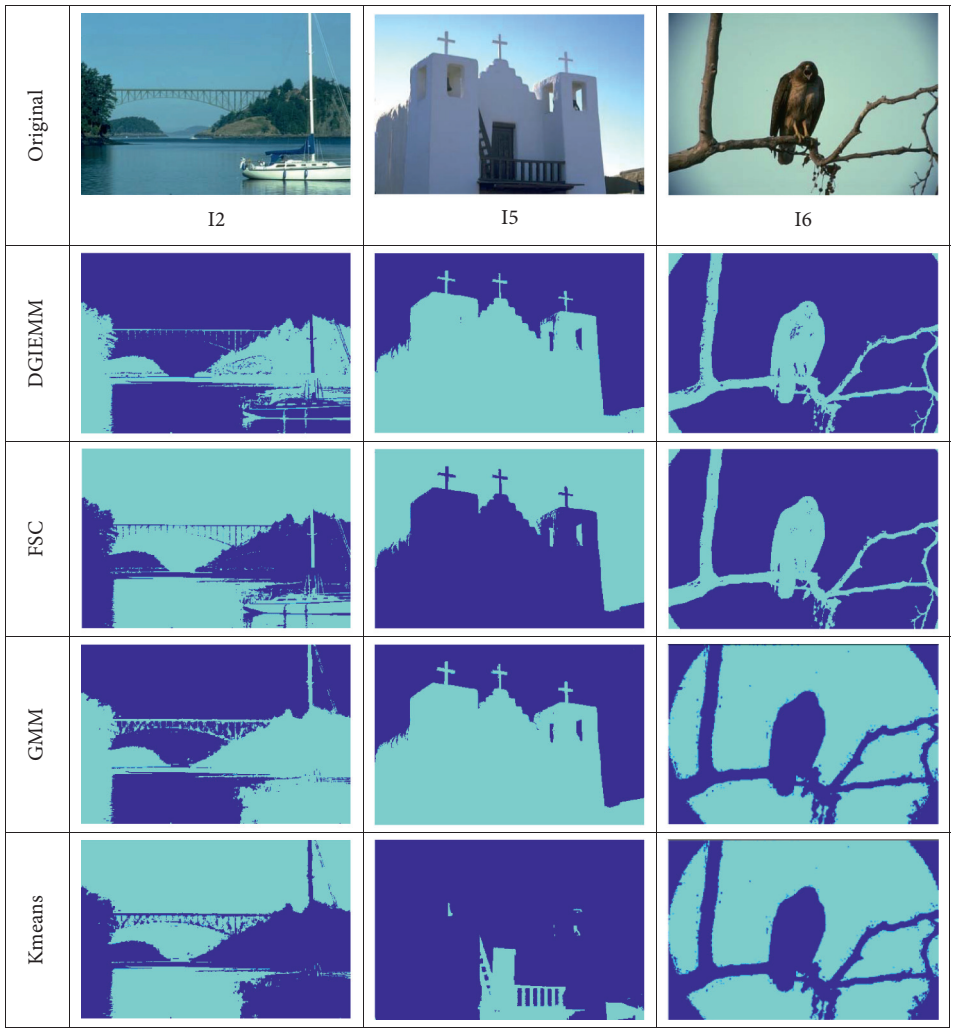

Figure 8: Segmented images (I1, I5, I6) using competitive algorithms.

where $\mathbf{n_{ij}}$ denotes the number of objects in common between classes. $\mathbf{a_i}$ and $\mathbf{b_i}$ are the sum of rows and columns of contingency table, respectively.

Hubert: it is a measure used to compute the correlation coefficient between classes and it is defined as:

$$\text{Hubert} = \frac{\mathring{a}_{i<j}\left(X_{ij}-\mu_X\right)\left(Y_{ij}-\mu_Y\right)}{N\,\sigma_X\sigma_Y}, \tag{40}$$

where $\sigma_{\mathbf{X}}$ and $\sigma_{\mathbf{Y}}$ are the standard deviation of cluster $\mathbf{X}$ and cluster $\mathbf{Y}$, respectively.

Normalized mutual information (NMI): is defined as a normalization of the Mutual Information that defined as:

$$\text{NMI} = \frac{2I\left(C_T; C\right)}{H\left(C_T\right) + H\left(C\right)}, \tag{41}$$

where $\mathbf{C_T}$ and $\mathbf{C}$ are the class label and its cluster label, respectively. $\mathbf{H}$ is the Entropy and Mutual Information between $\mathbf{C_T}$ and $\mathbf{C}$, respectively.

3.2.4. Results and Discussion. The comparison between the developed color image segmentation method (i.e., DGIEMM) and the other methods is given in Table 11. It can be noticed from these results the high ability of the developed method to cluster the images into their objects overall the other methods. For example, according to the results in

terms of accuracy, it can be seen from these values that the DGIEMM has a high ability to assign each pixel into its true label (i.e., the object that contains it). The FSC and GMM provide results better than K-means, and this observation can be noticed from Figure 7(a) that shows the average overall of the tested six images.

In terms of AR, it can be seen that the DGIEMM still provides results better than other methods. The same observations are noticed in the other three measures (i.e., RI, NMI, and Hubert); also, Figures 7(b)–7(d) shows the superiority of DGIEMM.

To justify the superiority of DGIEMM, the nonparametric Friedman test is used. In general, this test is applied to make a decision about the difference between the DGIEMM and other methods is significant or not. There are two hypotheses; the first one is named null, and it is assumed that there is no difference between the tested methods. In contrast, the second hypothesis, called alternative, is considered there is a difference between the method. We accept the alternative hypothesis, when the obtained value is less than significant level 0.05.

Table 12 shows the mean-rank obtained using the Friedman test in terms of the performance measures (i.e., accuracy, AR, RI, Hubert, NMI). From these values, it can be seen that the developed color image segmentation method has the highest mean rank in terms of performance measures. In addition, FSC allocates the second mean rank, followed by K-means that provides results better than traditional GMM. Finally, Figure 8 shows an example of Segmented image using competitive algorithms.

4. Concluding Remarks

In this study, a new two-parameters distribution for modeling a lot of observations in nature has been presented. It is constructed from continuous generalized inverted exponential distribution, so called discrete generalized inverted exponential distribution DGIE distribution. Some important probabilistic properties of this distribution have been studied. Using two methods namely the moment's method and the maximum likelihood technique, the parameters of the **DGIE**(β, θ) distribution have been estimated. To evaluate the quality of **DGIE**(β, θ), a set of experimental series has been conducted using synthetic and real data. The results have been shown the efficiency of **DGIE**(β, θ) in fitting data better than some existing distribution in case of synthetic data. In addition, the developed **DGIE** has been applied as image segmentation based on clustering technique, which aims to avoid the limitations of the traditional Gaussian mixture model (GMM). This is achieved by using **DGIE** instead of Gaussian distribution. The developed image segmentation has been established its performance using a set of color images which provides results better than GMM, K-means, and Fuzzy subspace clustering (FSC).

According to these properties and results, DGIE can be applied to a wide range of applications, including reliability, physics, and machine learning techniques.

Data Availability

The data used to support the findings of this study are available from the authors upon request.

Conflicts of Interest

The authors declare no conflict of interest.

References

[1] M. A. Ilani and M. Khoshnevisan, "Powder mixed-electrical discharge machining (EDM) with the electrode is made by fused deposition modeling (FDM) at Ti-6Al-4V machining procedure," *Multiscale and Multidisciplinary Modeling, Experiments and Design*, vol. 3, no. 3, pp. 173–186, 2020.

[2] N. H. Phan, V. N. Pi, N. Q. Tuan et al., "Tool wear rate analysis of uncoated and AlCrNi coated aluminum electrode in EDM for Ti-6Al-4 V titanium alloy," *Advances in Engineering Research and Application*, pp. 832–838, 2021.

[3] "Material removal rate during b4c abrasives mixed electrical discharge machining of titanium alloy (ti-6al-4v)," *International Journal of Latest Trends in Engineering and Technology*, vol. 7, no. 3, 2016.

[4] R. Kwitt, P. Meerwald, and A. Uhl, "Color-image watermarking using multivariate power-exponential distribution," in *Proceedings of the 2009 16th IEEE International Conference on Image Processing (ICIP)*, pp. 4245–4248, IEEE, Cairo, Egypt, 7 November 2009.

[5] M. A. Ilani and M. Khoshnevisan, "Study of surfactant effects on intermolecular forces (IMF) in powder-mixed electrical discharge machining (EDM) of Ti-6Al-4V," *International Journal of Advanced Manufacturing Technology*, vol. 116, no. 5-6, pp. 1763–1782, 2021.

[6] G. Paul, J. Cardinale, and I. F. Sbalzarini, "Coupling image restoration and segmentation: a generalized linear model/bregman perspective," *International Journal of Computer Vision*, vol. 104, no. 1, pp. 69–93, 2013.

[7] B. Ghoshal, A. Tucker, B. Sanghera, and W. Lup Wong, "Estimating uncertainty in deep learning for reporting confidence to clinicians in medical image segmentation and diseases detection," *Computational Intelligence*, vol. 37, no. 2, pp. 701–734, May 2021.

[8] M. A. Ilani and M. Khoshnevisan, "Mathematical and physical modeling of FE-SEM surface quality surrounded by the plasma channel within Al powder-mixed electrical discharge machining of Ti-6Al-4V," *International Journal of Advanced Manufacturing Technology*, vol. 112, no. 11-12, pp. 3263–3277, 2021.

[9] A. Taherkhani, M. A. Ilani, F. Ebrahimi et al., "Investigation of surface quality in Cost of Goods Manufactured (COGM) method of μ-Al2O3 Powder-Mixed-EDM process on machining of Ti-6Al-4V," *International Journal of Advanced Manufacturing Technology*, vol. 116, no. 5-6, pp. 1783–1799, 2021.

[10] W. Nelson, W. Q. Meeker, and L. A. Escobar, "Statistical methods for reliability data," *Technometrics*, vol. 40, no. 3, p. 255, 1998.

[11] S. Kotz, C. B. Read, N. Balakrishnan, B. Vidakovic, and N. L. Johnson, *Encyclopedia of Statistical Sciences*, John Wiley & Sons, Hoboken, NJ, USA, 2004.

[12] D. Roy and R. P. Gupta, "Classifications of discrete lives," *Microelectronics Reliability*, vol. 32, no. 10, pp. 1459–1473, Oct. 1992.
[13] D. Roy, "Reliability measures in the discrete bivariate set-up and related characterization results for a bivariate geometric distribution," *Journal of Multivariate Analysis*, vol. 46, no. 2, pp. 362–373, Aug. 1993.
[14] H. Krishna and P. Singh Pundir, "Discrete burr and discrete pareto distributions," *Statistical Methodology*, vol. 6, no. 2, pp. 177–188, 2009.
[15] B. A. Para and T. R. Jan, "Discrete generalized burr-type XII distribution," *Journal of Modern Applied Statistical Methods*, vol. 13, no. 2, pp. 244–258, 2014.
[16] B. A. Para and T. R. Jan, "Discrete inverse Weibull minimax distribution: properties and applications," *Journal of Statistics Applications & Probability*, vol. 6, no. 1, pp. 205–218, 2017.
[17] E. Gómez-Déniz and E. Calderín-Ojeda, "The discrete Lindley distribution: properties and applications," *Journal of Statistical Computation and Simulation*, vol. 81, no. 11, pp. 1405–1416, 2011.
[18] V. Nekoukhou and H. Bidram, "Exponential-discrete generalized exponential distribution: a new compound model," *Journal of Statistical Theory and Applications*, vol. 15, no. 2, p. 169, 2016.
[19] A. M. Abouammoh and A. M. Alshingiti, "Reliability estimation of generalized inverted exponential distribution," *Journal of Statistical Computation and Simulation*, vol. 79, no. 11, pp. 1301–1315, 2009.
[20] A. M. Abd-Elfattah, S. M. Assar, and H. I. Abd-Elghaffar, "Exponentiated generalized Frechet distribution," *Int. J. Math. Anal. Appl.*vol. 3, no. 5, pp. 39–48, 2016.
[21] S. Dey and T. Dey, "On progressively censored generalized inverted exponential distribution," *Journal of Applied Statistics*, vol. 41, no. 12, pp. 2557–2576, Dec. 2014.
[22] H. Krishna and K. Kumar, "Reliability estimation in generalized inverted exponential distribution with progressively type II censored sample," *Journal of Statistical Computation and Simulation*, vol. 83, no. 6, pp. 1007–1019, Jun. 2013.
[23] M. D. Nichols and W. J. Padgett, "A bootstrap control chart for Weibull percentiles," *Quality and Reliability Engineering International*, vol. 22, no. 2, pp. 141–151, 2006.
[24] E. Gómez-Déniz, "Another generalization of the geometric distribution," *Test*, vol. 19, no. 2, pp. 399–415, 2010.
[25] G. Blom, H. Linhart, and W. Zucchini, "Model selection," *Biometrics*, vol. 45, no. 1, p. 340, 1989.
[26] P. D. McNicholas and T. B. Murphy, "Parsimonious Gaussian mixture models," *Statistics and Computing*, vol. 18, no. 3, pp. 285–296, Sep. 2008.
[27] J. Diaz-Rozo, C. Bielza, and P. Larranaga, "Clustering of data streams with dynamic Gaussian mixture models: an IoT application in industrial processes," *IEEE Internet of Things Journal*, vol. 5, no. 5, pp. 3533–3547, Oct. 2018.
[28] L. Abualigah, A. Diabat, S. Mirjalili, M. Abd Elaziz, and A. H. Gandomi, "The arithmetic optimization algorithm," *Computer Methods in Applied Mechanics and Engineering*, vol. 376, Article ID 113609, 2021.
[29] X.-M. Zhao, "Bayesian information criterion (BIC)," in *Encyclopedia of Systems Biology*p. 73, Springer New York, New York, NY, 2013.
[30] L. Abualigah, M. A. Elaziz, P. Sumari, Z. W. Geem, and A. H. Gandomi, "Reptile Search Algorithm (RSA): a nature-inspired meta-heuristic optimizer," *Expert Systems with Applications*, vol. 191, Article ID 116158, 2022.
[31] D. Martin, C. Fowlkes, D. Tal, and J. Malik, "A database of human segmented natural images and its application to evaluating segmentation algorithms and measuring ecological statistics,"vol. 2, pp. 416–423, in *Proceedings of the Eighth IEEE International Conference on Computer Vision*, vol. 2, IEEE, Vancouver, BC, Canada, 7 July 2001.